CHEMISTRY OF MATERIALS
Article

Chem. Mater. **2009,** *21,* 5743–5753 5743
DOI:10.1021/cm902599w

Stereoregular Methacrylate-POSS Hybrid Polymers: Syntheses and Nanostructured Assemblies

Nicole C. Escudé and Eugene Y.-X. Chen*

Department of Chemistry, Colorado State University, Fort Collins, Colorado 80523-1872

Received August 23, 2009. Revised Manuscript Received October 27, 2009

This contribution reports the first examples of stereoregular (isotactic, *it*-, and syndiotactic, *st*-) methacrylate-POSS (polyhedral oligomeric silsesquioxane) hybrid polymers and their derived nanostructured assemblies. The polymerization of methyl methacrylate (MMA) by isospecific and syndiospecific living metallocene catalysts, when end-capped with methacrylisobutyl POSS (MA-POSS) or simultaneously copolymerized with MA-POSS at ambient temperature, readily produces highly stereoregular (94% *it*- and *st*-) MA-POSS end-capped PMMA (PMMA-POSS) or statistical copolymers PMMA-*co*-P(MA-POSS). The MA-POSS incorporation in the *it*-copolymers ranges from a low 2.6 mol % (20 wt %) to a high, maximum 24 mol % (75 wt %), whereas the incorporation in the *st*-copolymers is relatively lower with the same comonomer feed ratio due to the formation of a crystalline inclusion complex in which the POSS nanocages are encapsulated within the helical *st*-PMMA cavity. The *it*-copolymers with high POSS contents (> 20 mol %) show evidence for interchain association through POSS aggregation and display a ~20 °C T_g enhancement over the pristine *it*-PMMA. MA-POSS end-capped diastereomeric PMMAs exhibit versatile nanostructured assemblies, including micelle-like core−shell nanostructures (R_h up to 186 nm derived from the 5.7 nm *it*-PMMA-POSS unimer) through POSS inorganic collapse in selective solvents, helical stereocomplexes (R_h = 11 nm) between two or three polymer chains through organic self-organization of the diastereomeric PMMAs, and large core−shell nanospheres (R_h up to 636 nm) through synergistic organic PMMA self-organization and inorganic POSS nanocluster aggregation. Thermal annealing of the *it*-/*st*-PMMA-POSS blend in a 1:2 ratio also generates the crystalline stereocomplex with a high T_m of 213 °C.

Introduction

Hybrid polymers[1] are characterized as polymers containing organic and inorganic entities or domains covalently linked within the same polymer chains. Such polymers conceptually depart from conventional composite or hybrid materials comprising mixtures of organic polymers and inorganic phases that are physically blended together—the type of polymer composite materials that chemists and materials scientists have mostly focused on.[2] Unlike hybrid composite materials, the well-defined organic and inorganic entities within hybrid polymers can be precisely controlled at the molecular level; hence, it is anticipated that a multitude of unique and useful nanostructured assemblies will emerge therefrom, by virtue of synergistic inorganic collapse and organic self-organization phenomena occurring within the confined length scale.

Organic−inorganic hybrid materials based on the incorporation of inorganic ceramic-like, reinforcing "molecular silica" polyhedral oligomeric silsesquioxane (POSS) nanocages,[3] which can be dispersed on a molecular scale (1−3 nm) or as micrometer-size crystalline (or amorphous) aggregates into organic polymeric matrices, have attracted increasing attention in recent years due to the observed enhancements of such materials in a variety of physical and mechanical properties.[3−5] Methacrylate-POSS (MA-POSS) derived hybrid polymers[6] or hybrid composites[7] represent an important class of such advanced materials due to their enhanced thermal stability, increased glass-transition temperature (T_g) and oxygen

*Corresponding author. E-mail: eugene.chen@colostate.edu.

(1) Selected reviews on hybrid polymers: (a) George, S. M.; Yoon, B.; Dameron, A. A. *Acc. Chem. Res.* **2009**, *42*, 498–508. (b) Sanchez, C.; Boissière, C.; Grosso, D.; Laberty, C.; Nicole, L. *Chem. Mater.* **2008**, *20*, 682–735. (c) Greenham, N. C. In *Organic Photovoltaics*; Brabec, C. J.; Dyakonov, V.; Scherf, U., Eds.; Wiley-VCH: Weinheim, Germany, 2008; Chapter 6, pp 179−210. (d) Rehahn, M. *Acta Polym.* **1998**, *49*, 201–224.

(2) Selected reviews on hybrid nanocomposites: (a) Paul, D. R.; Robeson, L. M. *Polymer* **2008**, *49*, 3187–3204. (b) Costa, F. R.; Saphiannikova, M.; Wagenknecht, U.; Heinrich, G. *Adv. Polym. Sci.* **2008**, *210*, 101–168. (c) Schaefer, D. W.; Justice, R. S. *Macromolecules* **2007**, *40*, 8501–8517. (d) Moniruzzaman, M.; Winey, K. I. *Macromolecules* **2006**, *39*, 5194–35205. (e) Sanchez, C.; Julián, B.; Belleville, P.; Popall, M. *J. Mater. Chem.* **2005**, *15*, 3359–3592. (f) Bockstaller, M. R.; Mickiewicz, R. A.; Thomas, E. L. *Adv. Mater.* **2005**, *17*, 1331–1349. (g) Ray, S. S.; Okamoto, M. *Prog. Polym. Sci.* **2003**, *28*, 1539–1641. (h) *Polymer Nanocomposites: Synthesis, Characterization, and Modeling*; Krishnamoorti, R.; Vaia, R. A. Eds.; ACS Symposium Series; American Chemical Society: Washington, DC, 2002; Vol. *804*. (i) Schmidt, D.; Shah, D.; Giannelis, E. P. *Curr. Opin. Solid State Mater. Sci.* **2002**, *6*, 205–212. (j) Manias, E.; Touny, A.; Wu, L.; Strawhecker, K.; Lu, B.; Chung, T. C. *Chem. Mater.* **2001**, *13*, 3516–3523. (k) *Polymer−Clay Nanocomposites*; Pinnavaia, T. J.; Beall, G. W. Eds.; Wiley: New York, 2000. (l) Alexandre, M.; Dubois, P. *Mater. Sci. Eng., R* **2000**, *28*, 1–63.

Published on Web 11/12/2009

permeability, reduced flammability and heat evolution, modified mechanical properties, as well as improved toughness,[3i,6f,6g,6u,7a,7c,7d] when compared to the homologous pristine poly(methyl methacrylate), PMMA. However, all current MA-POSS hybrid polymers were produced exclusively from various radical polymerization processes[6] that typically afford essentially atactic or syndio-rich polymers. It is well-established that the physical and mechanical properties of methacrylate polymers depend largely on their stereochemistry;[8] stereoregular polymers typically have superior materials properties, such as enhanced solvent resistance and high modulus as well as excellent impact strength and fatigue resistance, in comparison to their amorphous counterparts. Hence, it is of fundamental interest to investigate effects of stereomicrostructures and their derived nanostructures of the MA-POSS hybrid polymers on their materials properties, key components in the study of structure−property relationships for the POSS-based hybrid polymers. The challenge here, however, has been in the synthesis of the POSS-containing methacrylate polymers with not only well-defined chain structures but also programmable stereomicrostructures.

The recently developed coordination, living, and stereospecific polymerization of methacrylates with group 4 chiral metallocene ester enolate and related catalysts offers a great advantage over traditional radical, anionic, or group-transfer polymerization techniques in terms of its ability to control the stereochemistry of the polymerization, in addition to its high degree of control over polymerization at ambient temperature.[9] Thus, using appropriate chiral metallocene catalysts, we have synthesized the following methacrylate polymers with well-defined polymer chain structures (e.g., polymers with controlled molecular weight, MW, and narrow MW distribution, MWD) and stereomicrostructures (tacticities and chiroptical activities): highly isotactic (*it*-) PMMA ([*mm*] ≥ 95%) and *it*-PBMA [poly(*n*-butyl methacrylate), [*mm*] > 99%],[10,11] highly syndiotactic (*st*-) PMMA ([*rr*] = 94%),[12] isotactic-*b*-syndiotactic stereo(di)block (*sb*-) PMMA ([*mm*] = 45.7%, [*mr*] = 7.9%, [*rr*] = 46.4%)[13] and stereo(multi)block *sb*-PMMA,[14,15] as well as optically active copolymers of MMA with *N*,*N*-diaryl acrylamides that render solution-stable, rigid, single-handed helical secondary structures.[16,17] These stereomicrostructures

(3) Selected reviews on POSS-based polymers and composites: (a) Wu, J.; Mather, P. T. *Polym. Rev.* **2009**, *49*, 25–63. (b) Pielichowski, K.; Njuguna, J.; Janowski, B.; Pielichowski, J. *Adv. Polym. Sci.* **2006**, *201*, 225–296. (c) Kannan, R. Y.; Salacinski, H. J.; Butler, P. E.; Seifalian, A. M. *Acc. Chem. Res.* **2005**, *38*, 879–884. (d) Li, G. Z.; Pittman, C. U., Jr. In *Macromolecules Containing Metals and Metal-like Elements*; Abd El Aziz, A. S.; Carraher, C. E.; Pittman, C. U., Jr.; Zeldin, M., Eds.; John Wiley & Sons: Hoboken, NJ, 2005; Vol.*4*, Chapter 5, pp 79−131. (e) Phillips, S. H.; Haddad, T. S.; Tomczak, S. J. *Curr. Opin. Solid State Mater. Sci.* **2004**, *8*, 21–29. (f) Li, G. Z.; Wang, L. C.; Ni, H. L.; Pittman, C. U., Jr.; Inorg, J. *Organomet. Polym.* **2001**, *11*, 123–154. (g) Pyun, J.; Matyjaszewski, K. *Chem. Mater.* **2001**, *13*, 3436–3448. (h) Sanchez, C.; de A. A. Soler-Illia, G. J.; Ribot, F.; Lalot, T.; Mayer, C. R.; Cabuil, V. *Chem. Mater.* **2001**, *13*, 3061–3083. (i) Schwab, J. J.; Lichtenhan, J. D. *Appl. Organomet. Chem.* **1998**, *12*, 707–713. (j) Lichtenhan, J. D. *Comm. Inorg. Chem.* **1995**, *17*, 115–130.

(4) Selected examples of Olefin-POSS hybrid polymers: (a) Zhang, H.-X.; Jung, M.-S.; Shin, Y.-J.; Yoon, K.-B.; Lee, D.-H. *J. Appl. Polym. Sci.* **2009**, *111*, 2697–2702. (b) Zhang, H.-X.; Shin, Y.-J.; Yoon, K.-B.; Lee, D.-H. *Eur. Polym. J.* **2009**, *45*, 40–46. (c) Seurer, B.; Coughlin, E. B. *Macromol. Chem. Phys.* **2008**, *209*, 1198–1209. (d) Zhang, H.-X.; Lee, H.-Y.; Shin, Y.-J.; Yoon, K.-B.; Noh, S.-K.; Lee, D.-H. *Polym. Int.* **2008**, *57*, 1351–1356. (e) Misra, R.; Fu, B. X.; Morgan, S. E. *J. Polym. Sci., Part B: Polym. Phys.* **2007**, *45*, 2441–2455. (f) Wang, J.; Ye, Z.; Joly, H. *Macromolecules* **2007**, *40*, 6150–6163. (g) Zheng, L.; Hong, S.; Cardoen, G.; Burgaz, E.; Gido, S. P.; Coughlin, E. B. *Macromolecules* **2004**, *37*, 8606–8611. (h) Zheng, L.; Kasi, R. M.; Farris, R. J.; Coughlin, E. B. J. *Polym. Sci. Part A: Polym. Chem.* **2002**, *40*, 885–891. (i) Zheng, L.; Farris, R. J.; Coughlin, E. B. *Macromolecules* **2001**, *34*, 8034–8039. (j) Jeon, H. G.; Mather, P. T.; Haddad, T. S. *Polym. Int.* **2000**, *49*, 453–457. (k) Tsuchida, A.; Bolln, C.; Sernetz, F.; G.; Frey, H.; Mülhaupt, R. *Macromolecules* **1997**, *30*, 2818–2824.

(5) Selected examples of Olefin-POSS hybrid blends: (a) Misra, R.; Fu, B. X.; Morgan, S. E. *J. Polym. Sci., Part B: Polym. Phys.* **2007**, *45*, 2441–2455. (b) Pracella, M.; Chionna, D.; Fina, A.; Tabuani, D.; Frache, A.; Camino, G. *Macromol. Symp.* **2006**, *234*, 59–67.

(6) Selected examples of Methacrylate-POSS hybrid polymers: (a) Liu, L.; Wang, W. *Polym. Bull.* **2009**, *62*, 315–325. (b) Garcia, O.; Sastre, R.; Garcia-Moreno, I.; Martin, V.; Costela, A. *J. Phys. Chem. C* **2008**, *112*, 14710–14713. (c) Markovic, E.; Clarke, S.; Matisons, J.; Simon, G. P. *Macromolecules* **2008**, *41*, 1685–1692. (d) Liu, Y.-L.; Tseng, M.-C.; Fangchiang, M-H. J. *Polym. Sci. Part A: Polym. Chem.* **2008**, *46*, 5157–5166. (e) Kotal, A.; Si, S.; Paira, T. K.; Mandal, T. K. *J. Polym. Sci., Part A: Polym. Chem.* **2008**, *46*, 1111–1123. (f) Zhao, C.; Yang, X.; Wu, X.; Liu, X.; Wang, X.; Lu, L. *Polym. Bull.* **2008**, *60*, 495–505. (g) Xu, H.; Yang, B.; Wang, J.; Guang, S.; Li, C. *J. Polym. Sci., Part A: Polym. Chem.* **2007**, *45*, 5308–5317. (h) Amir, N.; Levina, A.; Silverstein, M. S. *J. Polym. Sci., Part A: Polym. Chem.* **2007**, *45*, 4264–4275. (i) Augustine, B. H.; Hughes, W. C.; Zimmermann, K. J.; Figueiredo, A. J.; Guo, X.; Chusuei, C. C.; Maidment, J. S. *Langmuir* **2007**, *23*, 4346–4350. (j) Chen, R.; Feng, W.; Zhu, S.; Botton, G.; Ong, B.; Wu, Y. *Polymer* **2006**, *47*, 1119–1123. (k) Bizet, S.; Galy, J.; Gérard, J.-F. *Macromolecules* **2006**, *39*, 2574–2583. (l) Huang, C.-F.; Kuo, S.-W.; Lin, F.-J.; Huang, W.-J.; Wang, C.-F.; Chen, W.-Y.; Chang, F.-C. *Macromolecules* **2006**, *39*, 300–308. (m) Patel, R. R.; Mohanraj, R.; Pittman, C. U., Jr. *J. Polym. Sci., Part B: Polym. Phys.* **2006**, *44*, 234–248. (n) Li, G. Z.; Cho, H.; Wang, L.; Toghiani, H.; Pittman, C. U., Jr. *J. Polym. Sci., Part A: Polym. Chem.* **2005**, *43*, 355–372. (o) Anderson, S. E.; Baker, E. S.; Mitchell, C.; Haddad, T. S.; Bowers, M. T. *Chem. Mater.* **2005**, *17*, 2537–2545. (p) Kopesky, E.; Cohen, R. E.; McKinley, G. H. *Macromolecules* **2004**, *37*, 8992–9004. (q) Ohno, K.; Sugiyama, S.; Koh, K.; Tsujii, Y.; Fukuda, T.; Yamahiro, M.; Oikawa, H.; Yamamoto, Y.; Ootake, N.; Watanabe, K. *Macromolecules* **2004**, *37*, 8517–8522. (r) Pyun, J.; Matyjaszewski, K.; Wu, J.; Kim, G.-M.; Chun, S. B.; Mather, P. T. *Polymer* **2003**, *44*, 2739–2750. (s) Zhang, W.; Fu, b. X.; Seo, Y.; Schrag, E.; Hsiao, B.; Mather, P. T.; Yang, N.-L.; Xu, D.; Ade, H.; Rafailovich, M.; Sokolov, J. *Macromolecules* **2002**, *35*, 8029–8038. (t) Pyun, J.; Matyjaszewski, K. *Macromolecules* **2000**, *33*, 217–220. (u) Lichtenhan, J. D.; Otonari, Y. A.; Carr, M. J. *Macromolecules* **1995**, *28*, 8435–8437.

(7) Selected examples of Methacrylate-POSS hybrid blends: (a) Feng, Y.; Jia, Y.; Xu, H. *J. Appl. Polym. Sci.* **2009**, *111*, 2684–2690. (b) Yen, Y.-C.; Kuo, S.-W.; Huang, C.-F.; Chen, J.-K.; Chang, F.-C. *J. Phys. Chem. B* **2008**, *112*, 10821–10829. (c) Weickmann, H.; Delto, R.; Thomann, R.; Brenn, R.; Döll, W.; Mülhaupt, R. *J. Mater. Chem.* **2007**, *42*, 87–92. (d) Kopesky, E. T.; McKinley, G. H.; Cohen, R. E. *Polymer* **2006**, *47*, 299–309. (e) Kopesky, E. T.; Boyes, S. G.; Treat, N.; Cohen, R. E.; McKinley, G. H. *Rheol. Acta* **2006**, *45*, 971–981.

(8) (a) Novak, R. W.; Lesko, P. M. Methacryllic Polymers. In *Kirk-Othmer Encyclopedia of Chemical Technology*, 4th ed.; Howe-Grant, M., Ed.; John Wiley and Sons: New York, 1995: Vol. *16*, pp 501−537. (b) Hatada, K.; Kitayama, T.; Ute, K. *Prog. Polym. Sci.* **1988**, *13*, 189–276. (c) Van Beylen, M.; Bywater, S.; Smets, G.; Szwarc, M.; Worsfold, D. J. *Adv. Polym. Sci.* **1988**, *86*, 87–143.

(9) Chen, E. Y.-X. *Chem. Rev.* **2009**, *109*, 10.1021/cr9000258.

(10) Bolig, A. D.; Chen, E. Y.-X. *J. Am. Chem. Soc.* **2004**, *126*, 4897–4906.

(11) Rodriguez-Delgado, A.; Chen, E. Y.-X. *Macromolecules* **2005**, *38*, 2587–2594.

(12) Ning, Y.; Chen, E. Y.-X. *J. Am. Chem. Soc.* **2008**, *130*, 2463–2465.

(13) Bolig, A. D.; Chen, E. Y.-X. *J. Am. Chem. Soc.* **2002**, *124*, 5612–5613.

(14) Chen, E. Y.-X.; Cooney, M. J. *J. Am. Chem. Soc.* **2003**, *125*, 7150–7151.

(15) Ning, Y.; Chen, E. Y.-X. *Macromolecules* **2006**, *39*, 7204–7215.

(16) Miyake, G. M.; Mariott, W. R.; Chen, E. Y.-X. *J. Am. Chem. Soc.* **2007**, *129*, 6724–6725.

(17) Miyake, G. M.; Chen, E. Y.-X. *Macromolecules* **2008**, *41*, 3405–3416.

are required for the construction of methacrylate polymers having higher order stereoregularity or unique morphologies, such as crystalline helical stereocomplex (*sc*-) PMMA through self-assembling stereocomplexation between diastereomeric *it*-/*st*-PMMA blends in a typical 1/2 ratio (or covalently linked *sb*-PMMA) either in the solid state, when annealed, or in suitable solvents, when crystallized.[18] In this context, we have also fabricated supramolecular *sc*-PMMA/silicate nanocomposites[19] by mixing dilute THF solutions of in situ polymerized diastereomeric PMMA/exfoliated silicate nanocomposites, *it*-/*st*-PMMA/silicates,[20] in a 1:2 ratio, followed by reprecipitation or crystallization procedures. Significantly, the resulting crystalline *sc*-PMMA matrix is resistant to boiling-THF or acetone extraction, and the *sc*-nanocomposite exhibits a high melting-transition temperature (T_m) of 201 or 210 °C, depending on the preparation procedure, which is in sharp contrast to the diastereomeric nanocomposite constituents, the matrix of which can be extracted out with the same solvents and exhibits no apparent T_m by differential scanning calorimetry (DSC) under the same DSC experiment methods.

Adhering to the research needs or current challenges of the field identified in the above overview, the research described herein focuses on two new aspects of the MA-POSS hybrid polymers: synthesis of stereoregular polymers and study of their thermodynamically driven nanostructured assemblies. We reasoned that the stereochemically controlled MA-POSS hybrid polymers, which were previously unavailable or inaccessible by conventional methods, could be synthesized using chiral metallocene catalysts that have been proven to be stereospecific and living polymerization catalysts for methacrylic monomers.[9] We further reasoned that the combined organic methacrylate molecular recognition (due to main-chain chirality) and inorganic POSS aggregation could present an attractive means for creating emerging nanostructures from such stereoregular MA-POSS hybrid polymers. This contribution reports our findings on these two fronts.

Experimental Section

Materials, Reagents, and Methods. All syntheses and manipulations of air- and moisture-sensitive materials were carried out in flamed Schlenk-type glassware on a dual-manifold Schlenk line, a high-vacuum line, or in an argon or nitrogen-filled glovebox. NMR-scale (typically in a 0.02 mmol scale) reactions were conducted in Teflon-valve-sealed J. Young-type NMR tubes. HPLC-grade organic solvents were sparged extensively with nitrogen during filling of the solvent reservoir and then dried by passage through activated alumina (for Et_2O, THF, and CH_2Cl_2) followed by passage through Q-5-supported copper catalyst (for toluene and hexanes) stainless steel columns. Benzene, Benzene-d_6 and toluene-d_8 were degassed, dried over sodium/potassium alloy and vacuum-distilled or filtered, whereas $CDCl_3$ and CD_2Cl_2 were dried over activated Davison 4 Å molecular sieves. NMR spectra were recorded on either a Varian Inova 300 (FT 300 MHz, ^{1}H; 75 MHz, ^{13}C; 282 MHz, ^{19}F) or a Varian Inova 400 spectrometer. Chemical shifts for ^{1}H and ^{13}C spectra were referenced to internal solvent resonances and are reported as parts per million relative to tetramethylsilane, whereas ^{19}F NMR spectra were referenced to external $CFCl_3$.

MMA (Aldrich Chemical Co.) was first degassed and dried over CaH_2 overnight, followed by vacuum distillation, and final purification involved titration with neat tri(*n*-octyl)aluminum (Strem Chemicals) to a yellow end point[21] followed by vacuum distillation. Methacrylisobutyl polyhedral oligomeric silsesquioxane (^{i}Bu$_7$Si$_8$O$_{12}$ propyl methacrylate, MA-POSS) was purchased from Hybrid Plastics and recrystallized from acetone prior to use. The purified monomers were stored in brown bottles in an inert glovebox at room temperature (MA-POSS) or at −30 °C (MMA) inside a glovebox freezer. Butylated hydroxytoluene (BHT-H, 2,6-di-*tert*-butyl-4-methylphenol) was purchased from Aldrich Chemical Co. and recrystallized from hexanes. Tris(pentafluorophenyl)borane $B(C_6F_5)_3$ and trityl tetrakis(pentafluorophenyl)borate $[Ph_3C][B(C_6F_5)_4]$ were obtained as a research gift from Boulder Scientific Co.; $B(C_6F_5)_3$ was further purified by recrystallization from hexanes at −30 °C, whereas $[Ph_3C][B(C_6F_5)_4]$ was used as received. The $THF\cdot B(C_6F_5)_3$ adduct was prepared by addition of THF to a toluene solution of the borane followed by removal of the volatiles and drying in vacuo. Literature procedures were employed for the preparation of the following chiral metallocene catalysts or precatalysts: *rac*-(EBI)ZrMe[OC(O^iPr)=CMe$_2$]$_2$ [EBI = $C_2H_4(\eta^5$-indenyl)$_2$],[10] *rac*-(EBI)Zr(THF)[OC(O^iPr)=CMe$_2$]$^+$[MeB(C_6F_5)$_3$]$^-$ (**1**),[10] (CGC)TiMe$_2$ [CGC = Me$_2$Si(η^5-(Me$_4$C$_5$)(^{t}BuN)],[22] (CGC)TiMe$^+$[MeB(C_6F_5)$_3$]$^-$ (**2**),[23] Ph$_2$C(Cp)(Flu)ZrMe[OC(O^iPr)=CMe$_2$] (Cp = η^5-cyclopentadienyl, Flu = η^5-fluorenyl),[12] Ph$_2$C(Cp)(Flu)Zr[OC(O^iPr)=CMe$_2$]$_2$,[12] and Ph$_2$C(Cp)(Flu)Zr(THF)[OC(O^iPr)=CMe$_2$]$^+$[MeB(C_6F_5)$_3$]$^-$ (**3**).[12]

General Polymerization Procedures. Polymerizations were performed in 30-mL oven-dried glass reactors inside an argon-filled glovebox at ambient temperature. In a typical procedure for statistical copolymerizations, predetermined amounts of $THF\cdot B(C_6F_5)_3$ and the appropriate precatalyst (i.e., the neutral dimethyl or monomethyl monoester enolate metallocene complex) in a 1:1 molar ratio were premixed in 5 mL of CH_2Cl_2 and stirred for 10 min to cleanly generate the corresponding cationic catalyst.[11] MA-POSS was first dissolved in MMA, and this monomer mixture was quickly added via pipet to the vigorously stirring catalyst solution. The polymerization was allowed to

(18) Selected examples of PMMA stereocomplexes: (a) Kawauchi, T.; Kitaura, A.; Kumaki, J.; Kusanagi, H.; Yashima, E. *J. Am. Chem. Soc.* **2008**, *130*, 11889–11891. (b) Kumaki, J.; Kawauchi, T.; Okoshi, K.; Kusanagi, H.; Yashima, E. *Angew. Chem., Int. Ed.* **2007**, *46*, 5348–5351. (c) Kawauchi, T.; Kumaki, J.; Okoshi, K.; Yashima, E. *Macromolecules* **2005**, *38*, 9155–9160. (d) Serizawa, T.; Hamada, K.-I.; Akashi, M. *Nature* **2004**, *429*, 52–55. (e) Slager, J.; Domb, A. J. *Adv. Drug Delivery Rev.* **2003**, *55*, 549–583. (f) Serizawa, T.; Hamada, K.; Kitayama, T.; Fujimoto, N.; Hatada, K.; Akashi, M. *J. Am. Chem. Soc.* **2000**, *122*, 1891–1899. (g) Hatada, K.; Kitayama, T.; Ute, K.; Nishiura, T. *Macromol. Symp.* **1998**, *132*, 221–230. (h) te Nijenhuis, K. *Adv. Polym. Sci.* **1997**, *130*(67−81), 244–246. (i) Spevacek, J.; Schneider, B. *Adv. Colloid Interface Sci.* **1987**, *27*, 81–150.
(19) Mariott, W. R.; Escudé, N. C.; Chen, E. Y.-X. *J. Polym. Sci., Part A: Polym. Chem.* **2007**, *45*, 2581–2592.
(20) Mariott, W. R.; Chen, E. Y.-X. *J. Am. Chem. Soc.* **2003**, *125*, 15726–15727.
(21) Allen, R. D.; Long, T. E.; McGrath, J. E. *Polym. Bull.* **1986**, *15*, 127–134.
(22) (a) Carpentier, J.-F.; Maryin, V. P.; Luci, J.; Jordan, R. F. *J. Am. Chem. Soc.* **2001**, *123*, 898–909. (b) Stevens, J. C.; Timmers, F. J.; Wilson, D. R.; Schmidt, G. F.; Nickias, P. N.; Rosen, R. K.; Knight, G. W.; Lai, S. Eur. Pat. Appl. EP 0 416815 A2, **1991**.
(23) Chen, Y.-X.; Marks, T. J. *Organometallics* **1997**, *16*, 3649–3657.

proceed for the given time interval with continuous stirring. The amounts of catalyst (39.0 μmol) were fixed for all statistical copolymerizations, while the amounts of MA-POSS and MMA were adjusted according to the feed ratios specified in the polymerization table. For MMA polymerizations end-capping with MA-POSS, after in situ generation of the catalyst as described above, MMA was quickly added via pipet and vigorously stirred for 15 min (during which time all MMA was consumed) before the addition of the MA-POSS monomer; the reaction mixture was allowed to stir for 2 h at ambient temperature. After the measured time interval, a 0.2 mL aliquot was taken from the reaction mixture via syringe and quickly quenched into a 4 mL vial containing 0.6 mL of undried "wet" $CDCl_3$ stabilized by 250 ppm of BHT-H; the quenched aliquots were later analyzed by ^{1}H NMR to obtain monomer conversion data. After the removal of the aliquot, the polymerization was immediately quenched by addition of 5 mL 5% HCl-acidified methanol. The quenched mixture was precipitated into 100 mL of methanol, stirred for 1 h, filtered, washed with methanol followed by hexanes, and dried in a vacuum oven at 50 °C overnight to a constant weight. The MA-POSS incorporation in the copolymer or POSS end-capped PMMA samples was determined by analysis of ^{1}H NMR ($CDCl_3$) of the dried polymer samples, using integration of the PMMA peak at δ 3.60 ppm (s, 3H, OCH_3) and the POSS peak at δ 3.90 ppm (t, 2H, CH_2O). For samples with lower percentages of MA-POSS incorporation, it was sometimes necessary to use the more pronounced POSS peak at δ 0.63−0.59 ppm (dd, 16H, $SiCH_2$).

Polymer Characterizations. Gel permeation chromatography (GPC) and light scattering (LS) analyses of the polymers were carried out at 40 °C and a flow rate of 1.0 mL/min, with $CHCl_3$ as the eluent, on a Waters University 1500 GPC instrument equipped with four 5 μm PL gel columns (Polymer Laboratories) and calibrated using 10 PMMA standards or coupled with a Wyatt miniDAWN TREOS multiangle (45°, 90°, 135°) light scattering detector. GPC chromatograms were processed with Waters Empower software (version 2002); number-average molecular weight (M_n) and polydispersity index (M_w/M_n) of the polymers were given relative to PMMA standards. LS data were processed with Wyatt Astra Software (version 5.3.2.15) and dn/dc values were determined assuming 100% mass recovery of polymers with known concentrations.

Glass (T_g) and melting (T_m) transition temperatures of the polymer samples were measured by differential scanning calorimetry (DSC) on a DSC 2920 (TA Instruments). Polymer samples were first heated to 250 at 20 °C/min, equilibrated at this temperature for 4 min, then cooled to 25 at 20 °C/ min, held at this temperature for 4 min, and reheated to 300 at 10 °C/min. All T_g values were obtained from the second scan, while T_m values were recorded from the first scan (under the current, normal DSC conditions, no endotherms were observable from the second scans due to slow crystallization of PMMA). Maximum rate decomposition temperatures (T_{max}) and decomposition onset temperatures (T_{onset}) of the polymers were measured by thermal gravimetric analysis (TGA) on a TGA 2950 Thermogravimetric Analyzer, TA Instrument. Polymer samples were heated from ambient temperatures to 600 °C at a rate of 20 °C/ min. Values for T_{max} were obtained from derivative (wt%/°C) versus temperature (°C), whereas T_{onset} values (initial and end temperatures) were obtained from wt % versus temperature (°C) plots.

Dynamic light scattering (DLS) was used to determine the average hydrodynamic radii (R_h) of polymer samples.[24] The DLS analyses of the dilute polymer solutions (typically at 2×10^{-3} g/mL unless indicated otherwise) were performed on a DynaPro Titan (Wyatt Technology Corporation, model 803) equipped with a temperature controller and a 25 mW laser operating at λ = 826.6 nm, using Dynamics (Version 6) data collection and analysis software. The samples were gently warmed to quickly dissolve the polymer when using acetonitrile and xylenes solvents. The DLS measurements were conducted at 25 °C and a scattering angle of 90°, and the histograms were obtained by the averaging of ten runs, each run 10 s in duration.

Transmission electron microscopy (TEM) micrographs were obtained using a JEOL JEM-2000EXII transmission electron microscope operating at an accelerating voltage of 100 kV. The spacemen were dripped onto copper TEM grids (hexagonal 400 mesh) coated with a Formvar/carbon support film. After being fully dried on filter paper at room temperature, the spacemen were stained by exposure to osmium tetraoxide vapors (4% OsO_4 in water) overnight. MA-POSS end-capped *it*-PMMA samples were dissolved in CH_3CN or xylenes (40 mg/mL) by heating to 50 °C and then allowed to sit for 2 days before being filtered and dripped into TEM grids.

MA-POSS/*st*-PMMA Inclusion Complex Formation. Literature procedures for the formation of encapsulated fullerenes within the helical cavity of *st*-PMMA chains[25] were adopted for the encapsulation of the MA-POSS monomer molecules in *st*-PMMA helices. In a typical procedure, *st*-PMMA (20 mg) was added to a 1 mL solution of MA-POSS (10 mg) in either toluene or a mixture of toluene and 1,2-dichlorobenzene in a 1:1 volume ratio and fully dissolved upon heating to 110 °C. The solution was allowed to cool to room temperature and sit undisturbed overnight, after which the solution became a colorless, soft gel. After centrifugation for 10 min and subsequent removal of the supernatant by decantation, the gel was washed with the dissolution solvent and then recentrifuged. The inclusion complex was purified by repeating the above washing and centrifugation procedures four times.

Stereocomplex Formation and Characterizations. For stereocomplex formation via solution crystallization, 1 wt % solutions of *it*-PMMA-*co*-P(MA-POSS) and *st*-PMMA-*co*-P(MA-POSS) in THF (complexing solvent) were used. The solutions were combined in a typical 1:2 *it*-/*st*-PMMA-*co*-P(MA-POSS) ratio (or in other specified ratios) and allowed to stand undisturbed for 1 week. The precipitates were collected after filtration, washed, and dried in a vacuum oven. For stereocomplex formation by solid-state annealing, powdered *it*-PMMA-*co*-P(MA-POSS) and *st*-PMMA-*co*-P(MA-POSS) samples were combined in a specified ratio, pressed between two glass slides, and allowed to anneal in a 170 °C oven for a predetermined length of time (typically ~4 weeks). After stereocomplexation, the solid products were tested for insolubility in boiling acetone, and ^{1}H NMR in $CDCl_3$ (noncomplexing solvent) was used to determine overall stereocomplex tacticities. Thermal transitions (T_g and T_m) of the stereocomplexes were determined by DSC as described above.

Results and Discussion

Synthesis of Isotactic Methacrylate-POSS Copolymers and POSS End-Capped *it*-PMMA. Using living,

(24) (a) Berne, B. J.; Pecora, R. *Dynamic Light Scattering: with Applications to Chemistry, Biology, and Physics*; Dover Publications, Mineola, NY, 2000. (b) Chu, B. *Laser Light Scattering*; Academic Press: New York, 1991. (c) Schmitz, K. S. *An Introduction to Dynamic Light Scattering by Macromolecules*; Academic Press: San Diego, 1990.

(25) Kawauchi, T.; Kumaki, J.; Kitaura, A.; Okoshi, K.; Kusanagi, H.; Kobayashi, K.; Sugai, T.; Shinohara, H.; Yashima, E. *Angew. Chem., Int. Ed.* **2008**, *47*, 515–519.

Scheme 1. Synthesis of Isotactic Methacrylate-POSS Copolymers and POSS End-Capped *it*-PMMA

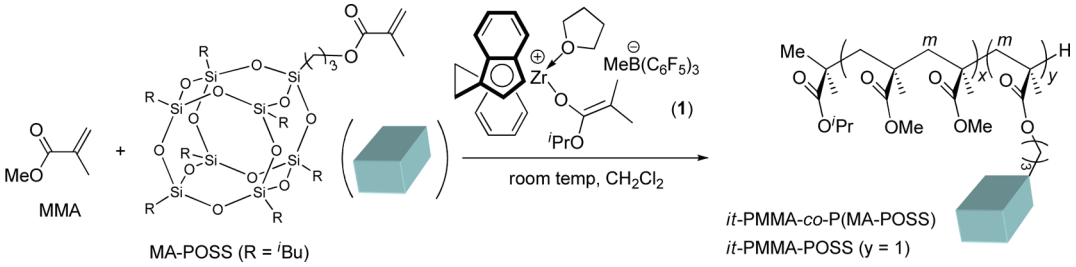

Table 1. Selected Results of Isospecific Copolymerization of MMA with MA-POSS by Catalyst 1[a]

				MA-POSS incorp.					
entry no.	MMA/ MA-POSS/**1**	time (h)	conv.[b] (%)	mol %	wt%	M_n[c] (kg/mol)	PDI[c] (M_w/M_n)	T_g[d] (°C)	[*mm*][b] (%)
1[e]	400:1.5:1	0.25/2	100	0.35	3.2	40.1	1.05	60	94
2	400:10:1	2	>99	2.6	20	52.1	1.03	56	91
3	400:60:1	3	>99	14	61	121	1.04	n.d.	92
4	400:70:1	3	>99	17	66	134	1.04	n.d.	92
5	400:100:1	4	>99	21	72	301	1.16	n.d.	93
6	400:150:1	4	78	24	75	850	1.27	74	n.d.

[a] Carried out in 5 mL of CH_2Cl_2 in an argon-filled glovebox at ambient temperature (~25 °C). [b] Monomer conversion, mol % MA-POSS incorporation, and isotacticity (methyl meso triad distribution) determined by ^{1}H NMR. [c] M_n and PDI determined by GPC relative to PMMA standards in $CHCl_3$. [d] T_g determined by DSC from second scans. [e] End-capping of the MMA polymerization by MA-POSS.

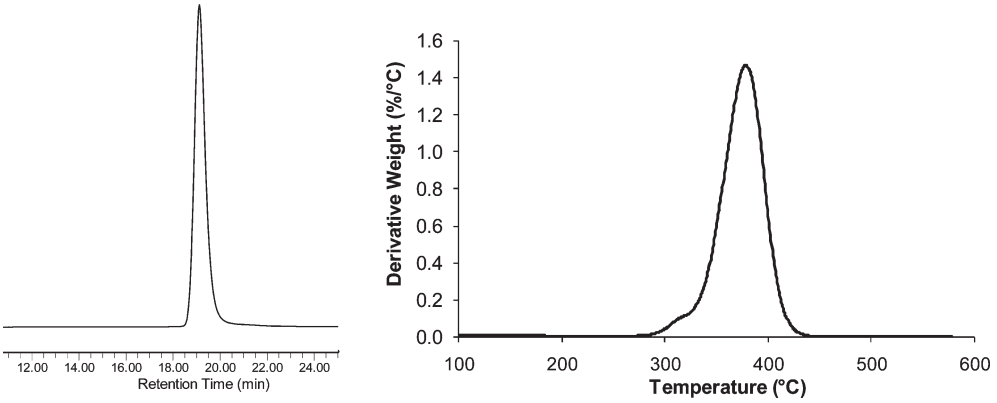

Figure 1. GPC (left column: $M_n = 5.21 \times 10^4$, $M_w/M_n = 1.03$) and TGA (right column: $T_{max} = 378.4$ °C) traces of *it*-PMMA-*co*-P(MA-POSS) (entry 2, Table 1).

isospecific, and coordination polymerization catalyst **1** with comonomers MMA and ^{i}Bu$_7$Si$_8$O$_{12}$-propyl methacrylate (a MA-POSS monomer containing the most common cubic octameric T_8−POSS nanobuilding block with the isobutyl peripheral substituents, Scheme 1), we have successfully synthesized a series of *it*-copolymers, *it*-PMMA-*co*-P(MA-POSS), having various levels of MA-POSS incorporation: from a low 0.35 mol % (3.2 wt %, MA-POSS end-capped *it*-PMMA, vide infra) to a high 24 mol % (75 wt %), Table 1. Because of the isospecific and living features of the methacrylate polymerization effected by catalyst **1**, the resulting POSS-containing copolymers with MA-POSS incorporation up to 21 mol % (entries 1−5, Table 1) exhibit high isotacticity ([*mm*] ≥ 91%), controlled M_n (by the initial monomer to catalyst ratio), narrow MWD (1.03−1.16), and defined end groups (the isobutyrate group is derived from the initiation by the ester enolate ligand of the catalyst and the H is derived from termination during workup by acidified methanol[11]). The MA-POSS incorporation increases almost linearly with an increase in the MA-POSS to MMA ratio in the initial feed. For example, the copolymerization in a 400:10:1 MMA:MA-POSS:**1** ratio (entry 2) achieved quantitative monomer conversion in 2 h at 25 °C and produced *it*-PMMA-*co*-P(MA-POSS) with $M_n = 5.21 \times 10^4$, $M_w/M_n = 1.03$ (Figure 1, left column), and MA-POSS incorporation = 2.6 mol % (20 wt %). TGA analysis (Figure 1, right column) of this sample reveled a T_{max} of 378.4 °C, T_{onset} of 349 °C (initial) and 400 °C (end), and a residue weight corresponding to the incorporated MA-POSS after the end T_{onset}. In comparison, the copolymerizations with 400:60:1 and 400:100:1 ratios afforded the copolymers with MA-POSS incorporation = 14 mol % (61 wt %, entry 3) and 21% (72 wt %, entry 5), respectively. The copolymerization with an even higher MA-POSS amount in the comonomer feed (e.g., in a 400:150:1 MMA:MA-POSS:**1** ratio, entry 6) did not achieved quantitative monomer conversion in 4 h and produced the copolymer with a broader MWD ($M_w/M_n = 1.27$). Nevertheless, the copolymer has

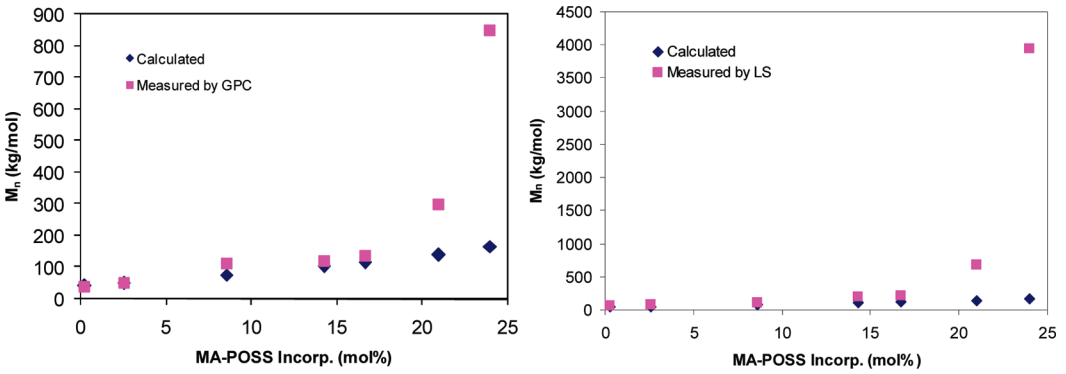

Figure 2. Comparisons between the measured M_n (by GPC relative to PMMA standards, left column; by light scattering, right column) and calculated M_n values of POSS-containing methacrylate polymers.

Scheme 2. Synthesis of Syndiotactic Methacrylate-POSS Copolymers and POSS End-capped *st*-PMMA

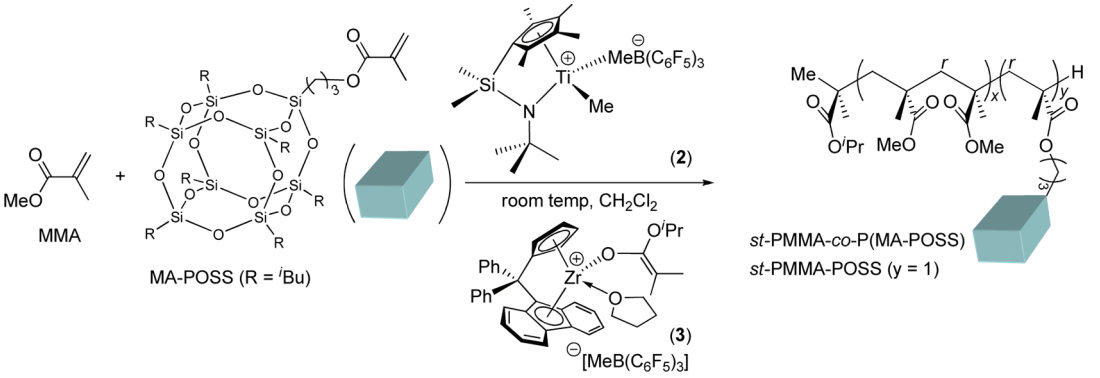

the highest level of MA-POSS incorporation of 24 mol % (75 wt %) and a high T_g of 74 °C, showing a ~20 °C enhancement over the T_g of the pristine *it*-PMMA (~55 °C[13]). The 24 mol % MA-POSS incorporation apparently represents a maximum level of incorporation by this catalyst under the current polymerization conditions as a further increase of MA-POSS in the feed did not enhance its incorporation in the copolymer product.

By polymerizing MMA first for 15 min (at which time all MMA had been consumed) and subsequently end-capping the living *it*-PMMA chain with the MA-POSS monomer, we also successfully synthesized POSS end-capped isotactic homopolymer *it*-PMMA-POSS (Scheme 1) having $M_n = 4.01 \times 10^4$ and $M_w/M_n = 1.05$ (entry 1, Table 1). This end-capping approach was successful because of the livingness of the PMMA chain and the inability of this catalyst to homopolymerize the bulky MA-POSS monomer.

The measured M_n values of these *it*-copolymers match well with the calculated M_n values for the copolymers with relatively lower percentages of MA-POSS incorporation (up to 17 mol %, Figure 2, left column), showing excellent control over polymer MW and MWD (≤1.05) under these conditions. However, The measured M_n values become much higher than the calculated ones for the copolymers with high MA-POSS incorporation (> 20 mol %, Figure 2, left column). This observation is viewed as evidence for interchain association in $CHCl_3$ through POSS aggregation for samples with high POSS contents, thus contributing to drastically increased hydrodynamic volumes corresponding to the much higher measured M_n values (e.g., $M_n = 8.50 \times 10^5$ when the MA-POSS incorporation reaches 24 mol %). Analysis of the copolymers with varied amounts of MA-POSS incorporation by light scattering revealed similar but more pronounced deviation of the measured M_w values from the calculated ones (Figure 2, right column; note that in this plot the measured M_w values were converted to M_n using PDI which ranged from 1.01 to 1.09 for the polymers analyzed here), again pointing to the interchain association (physical cross-linking) via POSS nanocage aggregation for polymers with high MA-POSS contents.

Synthesis of Syndiotactic Methacrylate-POSS Copolymers and POSS End-Capped *st*-PMMA. We employed two types of C_s-ligated metallocene catalysts for the synthesis of syndiotactic POSS-containing methacrylate polymers. First, (CGC)TiMe$^+$[MeB(C_6F_5)$_3$]$^-$ (**2**, Scheme 2) was used as it promotes living and syndioselective methacrylate polymerization at ambient[26] or higher[27] temperature. Indeed, end-capping of the syndiotactic living PMMA chain with the MA-POSS monomer afforded MA-POSS end-capped *st*-PMMA having $M_n = 4.52 \times 10^4$, $M_w/M_n = 1.07$, $T_g = 126$ °C, and $T_{max} = 390$ °C (entry 7, Table 2). This measured M_n is close to the calculated M_n of 4.16×10^4, giving excellent control of the polymerization with a high initiator

(26) Rodriguez-Delgado, A.; Mariott, W. R.; Chen, E. Y.-X. *Macromolecules* **2004**, *37*, 3092–3100.
(27) Lian, B.; Thomas, C. M.; Navarro, C.; Carpentier, J.-F. *Organometallics* **2007**, *26*, 187–195.

Table 2. Selected Results of Syndiospecific Copolymerization of MMA with MA-POSS by 2 and 3[a]

				MA-POSS incorp.						
entry no.	MMA/ MA-POSS/cat	time (h)	conv.[b] (%)	mol %	wt%	M_n[c] (kg/mol)	PDI[c] (M_w/M_n)	T_g[d] (°C)	T_{max}[e] (°C)	[*rr*][b] (%)
7[f]	400:1.5:1(**2**)	9/2	98	0.5	4.7	45.2	1.07	129	390	75
8	200:5:1(**2**)	25	91	2.2	17	26.1	1.11	n.d.	392	74
9	400:10:1(**2**)	36	96	1.3	11	46.0	1.10	n.d.	n.d.	74
10[f]	200:1.5:1(**3**)	0.25/4	85	~0.2	~1.9	26.7	1.28	134	391	93
11	200:5:1(**3**)	2	94	1.9	15	30.3	1.21	n.d.	389	94
12	400:10:1(**3**)	4	64	1.7	14	37.7	1.33	n.d.	n.d.	94

[a] Carried out in 10 mL of toluene with **2** or 5 mL of CH_2Cl_2 with **3**, in an argon-filled glovebox at ambient temperature (~25 °C). [b] Monomer conversion, mol % MA-POSS incorporation, and syndiotacticity (methyl racemic triad distribution) determined by ^{1}H NMR. [c] M_n and PDI determined by GPC relative to PMMA standards in $CHCl_3$. [d] T_g determined by DSC from second scans. [e] T_{max} determined by TGA. [f] End-capping of the MMA polymerization by MA-POSS.

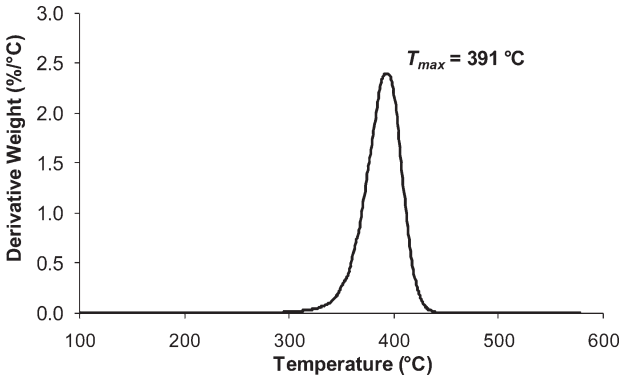

Figure 3. TGA derivative plot of *st*-PMMA-POSS (entry 10, Table 2).

efficiency {$I^* = M_n$(calcd)/M_n(exptl), where M_n(calcd) = MW(M) × [M]/[I] × conversion% + MW (chain-end groups)} of 92%. This titanium catalyst also enabled us to obtain syndiotactic copolymers *st*-PMMA-*co*-P(MA-POSS) with 2.2 mol % (17 wt %, entry 8) and 1.3 mol % (11 wt %, entry 9) MA-POSS incorporation, controlled by the initial comonomer feed ratio. Initiator efficiencies are also high (≥90%) for these statistical copolymerizations.

Catalyst **2** demonstrated remarkable control over polymer MW and MWD, but the polymer syndiotacticity is only modest (75% *rr*) and the polymerization activity is low. To produce *st*-copolymers with higher syndiotacticity and shorter reaction times, we next employed our recently developed, highly syndiospecific MMA polymerization catalyst $Ph_2C(Cp)(Flu)Zr(THF)[OC(O^iPr)=CMe_2]^+[MeB(C_6F_5)_3]^-$ (**3**, Scheme 2).[12] Gratifyingly, this catalyst afforded both end-capped *st*-PMMA (entry 10) and *st*-copolymers *st*-PMMA-*co*-P(MA-POSS) (entries 11 and 12) with high syndiotacticity of ≥93% within a 2−4 h reaction time period. Consistent with its high syndiotacticity, T_g of *st*-PMMA-POSS is relatively high (134 °C); the T_{max} of 391 °C (Figure 3) is more than 10 °C higher than the isotactic counterpart, but it is the same as the pristine *st*-PMMA.

Interestingly, the syndiospecific copolymerization of MMA with MA-POSS achieved a lower degree of MA-POSS incorporation relative to the isospecific one with the same comonomer feed ratio (e.g., entries 9 and 12 vs 2). In fact only a low level (3.7 mol %) of MA-POSS was incorporated even when the amount of MA-POSS was drastically increased in the copolymer feed to a ratio

Figure 4. Schematic representation of 1-D POSS arrays encapsulated within the helical *st*-PMMA cavity.

of [MMA]/[MA-POSS]/[Zr] = 200/30/1. A hypothesis is that *st*-PMMA chains can encapsulate MA-POSS monomer molecules within their large helical cavities (~1 nm) to form a crystalline inclusion complex in which the POSS nanocages are regulated into 1-D arrays encapsulated in the helices of the *st*-PMMA chains (Figure 4), resembling the peapod-like structure of the *st*-PMMA/C_{60} helical complex reported by Yashima et al.[25] This inclusion complex formation between the *st*-PMMA chains and the MA-POSS monomer molecules would hinder higher MA-POSS incorporation by depleting the comonomer and also sterically blocking access to the comonomer. Indeed, a polymer gel readily forms between *st*-PMMA and MA-POSS, containing up to 1.9 mol % (15 wt %) and 3.4 mol % (25 wt %) MA-POSS when prepared in toluene and toluene/*o*-dichlorobenzene, respectively, after removal of the excess, free MA-POSS (see Experimental Section). Unlike the pristine *st*-PMMA or the *st*-PMMA-*co*-MA-POSS copolymer of this study, which does not display significant or noticeable T_m under our current DSC methods (see Experimental Section), the crystalline inclusion complex exhibits either two large endothermic peaks on the first scan cycle (T_m = 131 °C, ΔH = 6.0 J/g; 156 °C, ΔH = 9.7 J/g; ΔH_{tot} = 15.7 J/g; Figure 5), for the complex prepared in toluene, or one endothermic peak (131 °C, ΔH = 16.5 J/g), for the complex prepared in toluene/*o*-dichlorobenzene. (Note that

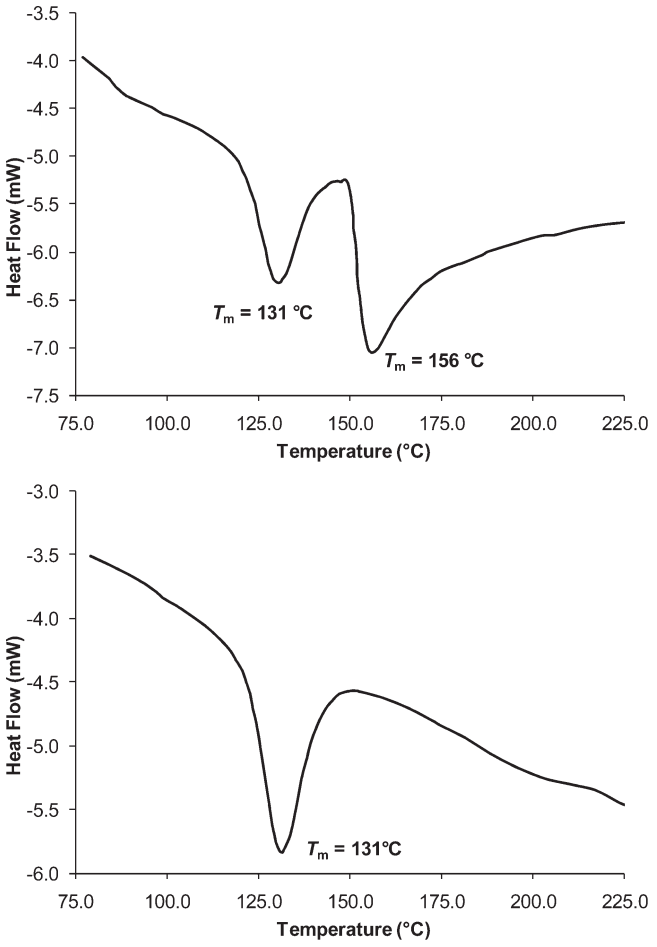

Figure 5. DSC traces of MA-POSS encapsulated *st*-PMMA crystalline inclusion complexes prepared in toluene (top: ΔH_{tot} = 15.7 J/g) and in toluene/*o*-dichlorobenzene (bottom: ΔH = 16.5 J/g).

the melting point of MA-POSS is ~111 °C.) The observation of the two endotherms for the crystalline inclusion complex prepared in toluene is attributable to the formation of two different crystallite domain morphologies, in analogy to the observed multiple endotherms for the stereocomplexes of PMMAs as a function of crystallization conditions.[28] Apparently, the ordered placement of the POSS nanocages within the *st*-PMMA cavity renders crystalline domains of the polymer. On the other hand, there is no such inclusion complex formation between *it*-PMMA and MA-POSS. These results provide strong evidence for the formation of such interesting crystalline inclusion complexes through molecular recognition.

Core−Shell Nanostructures via Inorganic or Organic Collapse. With POSS end-capped stereoregular PMMAs in hand, we employed DLS to investigate aggregation behavior of the POSS nanocages into nanoclusters (inorganic collapse) or association of methacrylate polymer chains (organic collapse) for the possible formation of micelle-like core−shell nanostructures in selective solvents. We reasoned that understanding of this process is the first step toward the construction of more complex nanostructured assemblies derived from stereoregular MA-POSS polymers with combined features of inorganic collapse and organic self-organization.

A THF solution of *it*-PMMA-POSS (run 1, Table 1) exhibits a monodisperse (polydispersity = 10.7%, i.e., less than a 20% cutoff for a monodisperse particle) particle size with an average R_h of 5.7 nm (Figure 6, left column) and no noticeable changes in the size and distribution while monitoring of this solution over 20 days. As THF (ε = 7.58) is a good solvent for both POSS and PMMA moieties, there exists no noticeable intra- or interchain aggregation, thereby giving rise to unassociated, individual polymer chains (i.e., unimers) in THF solution.

Switching to the less polar solvent xylenes (ε = 2.60), which is a nonselective solvent for either *it*-PMMA or POSS, generates a much larger structure having an average R_h of 26 nm (Figure 6, center column) after the polymer solution sat for 1 day at ambient temperature. As can be seen from the figure, the particle is uniform (no dispersity), but monitoring of this solution over a 1 day period showed time dependence of R_h and distribution before several size-distributed particles finally converged into the single, uniform particle shown in the figure. The resulting structure is characterized as a micelle with *it*-PMMA constituting the corona and POSS forming the core (see the TEM image in Figure 7).

Lastly, using a selective, polar solvent acetonitrile (ε = 37.5), which is a good solvent for *it*-PMMA but a poor solvent for POSS, we reasoned that we could generate micellar nanostructures with the POSS nanocages collapsing into a spherical (or cylindrical) core and the *it*-PMMA chains forming the shell. The DLS results are consistent with this reasoning. Thus, an acetonitrile solution of *it*-PMMA-POSS after 2 days at ambient temperature showed two types of micellar structures (Figure 6, right column). As in the case of the xylenes solution, the acetonitrile solution also showed, by monitoring of this solution over a 2 day period, time dependence of R_h and distribution before reaching the two unimodal size distributions shown in the figure after 2 days. The smaller but higher-mass-percentage structure (68 wt %) has an average R_h of 31 nm (no dispersity), corresponding to the core−shell micelle as described above, while the much larger but lower-mass percentage structure (32 wt %) has an average R_h of 186 nm (polydispersity = 17%), corresponding to intermicellar aggregates.

TEM micrographs of the *it*-PMMA-POSS sample prepared from xylenes solutions (40 mg/mL) after the solution sat at room temperature for 2 days show spherical micelles with the POSS core radius of ~100 nm for large particles (Figure 7a; the POSS-rich phase appears dark, as a result of selective staining by OsO_4[6r]). The much larger size observed by the TEM sample preparation techniques than those observed by the DLS solution techniques is presumably due to further aggregation during solvent evaporation process on the TEM grids and the use of 20 times higher concentration for TEM

(28) (a) Schomaker, E.; Hoppen, H.; Challa, G. *Macromolecules* **1988**, *21*, 2203–2209. (b) Schomaker, E.; Challa, G. *Macromolecules* **1988**, *21*, 2195–2203.

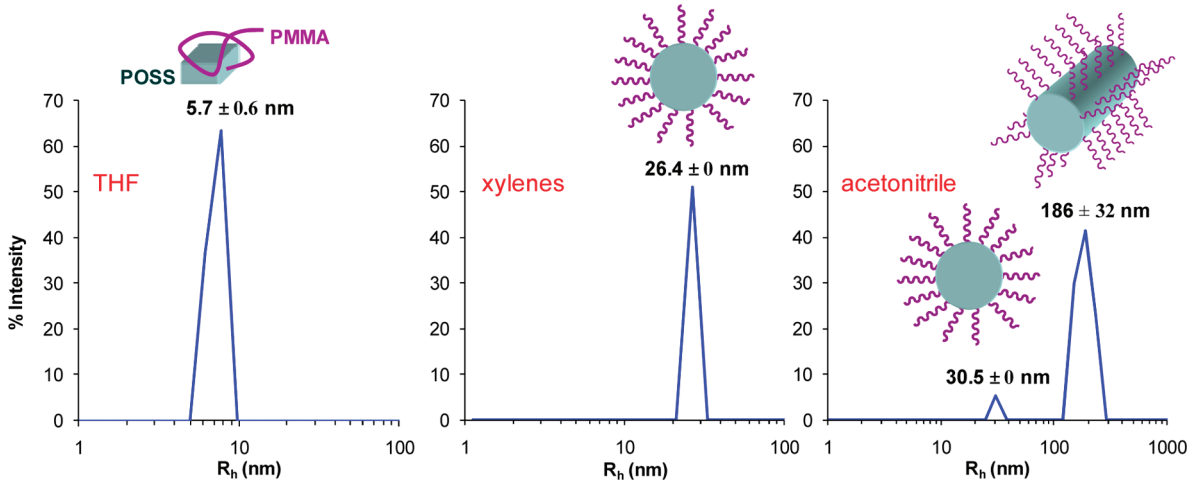

Figure 6. Size distributions (scattering intensity-weighted hydrodynamic radius R_h) of MA-POSS end-capped *it*-PMMA in selective solvents (2×10^{-3} g/mL) measured by DLS at RT.

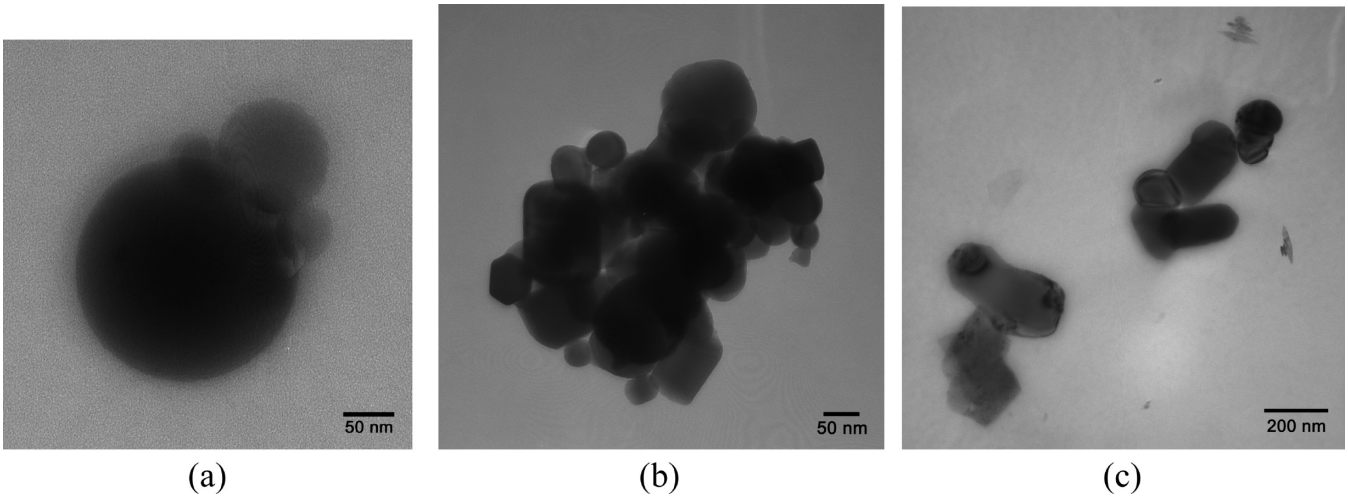

Figure 7. TEM images of *it*-PMMA-POSS as drop-cast xylenes (a) and acetonitrile (b) + (c) solutions (40 mg/mL) after they sat at room temperature for 2 days and subsequently stained with OsO_4.

sample preparation. TEM micrographs of the samples prepared in acetonitrile solutions under the same conditions show several types of micellar structures, including spherically, cubically, and cylindrically shaped POSS aggregates (Figure 7 b and c); the sizes of these micelles compare well to those observed in solutions by DLS (Figure 6). Overall, these TEM images qualitatively confirm the structures inferred from the DLS studies.

Stereocomplexes and Nanostructured Assemblies via Synergistic Organic Self-Organization and Inorganic Collapse. With diastereomeric PMMA chains end-capped with POSS and diastereomeric MMA copolymers with MA-POSS having approximately equally high degrees of stereoregularity (93% *mm* or *rr*) in hand, we investigated supramolecular stereocomplex formation via solution crystallization or solid-state annealing of physical blends of POSS end-capped PMMA *it*-/*st*-PMMA-POSS and random copolymers PMMA-*co*-P(MA-POSS).

We employed DLS to monitor stereocomplexation between *it*-/*st*-PMMA-POSS (1:2 ratio) in acetone, a complexing solvent for diastereomeric PMMA chains. Organic self-organization became apparent after 3 days for the 1 mg/mL solution, showing two monodisperse stereocomplex structures differing in size (Figure 8). The major (93.6 wt %) but smaller structure (R_h = 10.8 nm) can be characterized as a stereocomplex between two or three diastereomeric PMMA chains, considering that the R_h of the POSS end-capped unimer is ~5.7 nm (vide supra), whereas the minor (6.4 wt %) but larger structure (R_h = 26.9 nm) can be characterized as the associated stereocomplexed PMMA chains via POSS aggregation. Upon standing for 70 days, the size of the two structures remained relatively constant, whereas the weight percent of the larger structure increased considerably to 20.3 wt % (Figure 8).

A 10-fold increase of the concentration of the 1:2 blend (10 mg/mL) not only shortened the time for manifesting the stereocomplex formation, it also generated much larger structures (Figure 9). For example, sitting the solution for 2 days brought about two structures in a relatively close weight percent ratio: 86 nm R_h, 54.3 wt %; and 475 nm R_h, 45.7 wt %. After 9 days, the size of the smaller structure did not change noticeably, but the larger structure grew to a even larger aggregate (R_h = 636 nm,

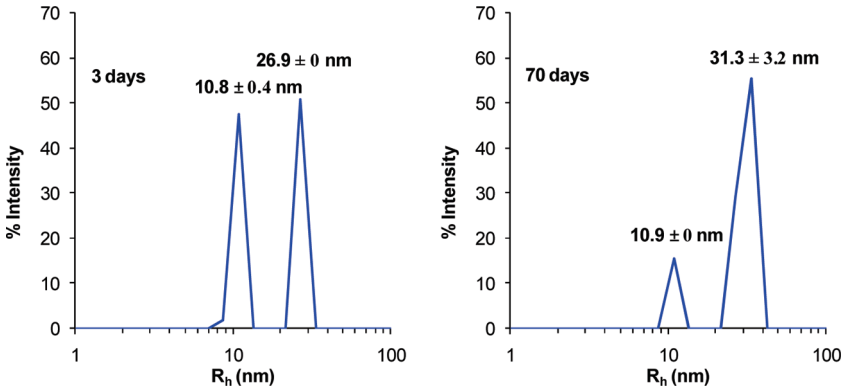

Figure 8. Size distributions (scattering intensity-weighted hydrodynamic radius R_h) of POSS end-capped *it*- and *st*-PMMAs in a 1/2 ratio in acetone (1×10^{-3} g/mL) after 3 and 70 days.

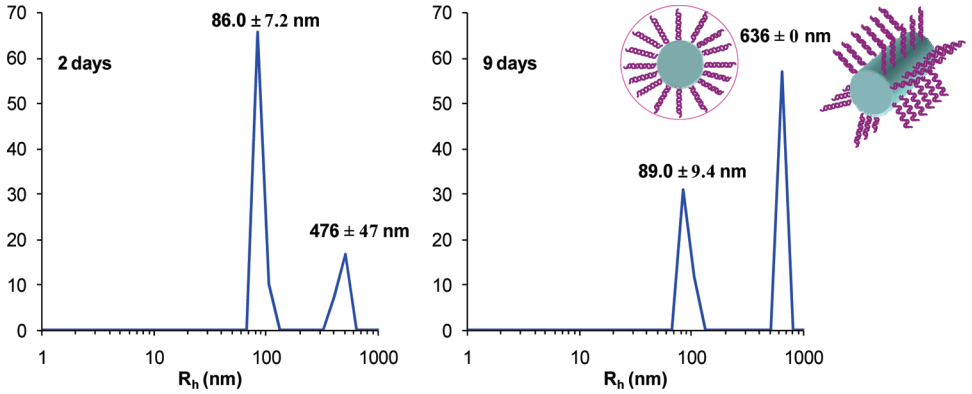

Figure 9. Size distributions (scattering intensity-weighted hydrodynamic radius R_h) of POSS end-capped *it*- and *st*-PMMAs in a 1:2 ratio in acetone (1×10^{-2} g/mL) after 2 and 9 days.

no dispersity) and became more pronounced in fraction (74.7 wt %). These results serve as evidence for formation of large nanostructured assemblies through synergistic organic self-organization, via stereocomplexation between diastereomeric PMMA chains, and inorganic collapse, via POSS association. Such proposed core−shell nanosphere structures with POSS as the spherical (or cylindrical) core and the stereocomplexed, double- or triple- stranded helical PMMA chains as the shell (Figure 9), where the larger structure corresponds to the intermicellar aggregate, resemble the core−shell nanospheres formed by simultaneously mixing C_{60} end-capped diastereomeric PMMA chains.[29]

Solid-state annealing of a physical blend of POSS end-capped PMMAs, *it*-/*st*-PMMA-POSS, in a 1:2 ratio at 170 °C for 4 weeks also generated the crystalline stereocomplex, as evidenced by a characteristically high T_m of 213 °C shown on its DSC trace (Figure 10). The stereocomplex formed is transparent and insoluble in boiling acetone, in contrast to the two constituent precursors, which are opaque and soluble in acetone at ambient temperature and do not exhibit T_m under the current DSC methods. Statistically enchained MA-POSS nanocages within the main chain significantly interrupt stereocomplexation as the thermally annealed 1:2 ratio

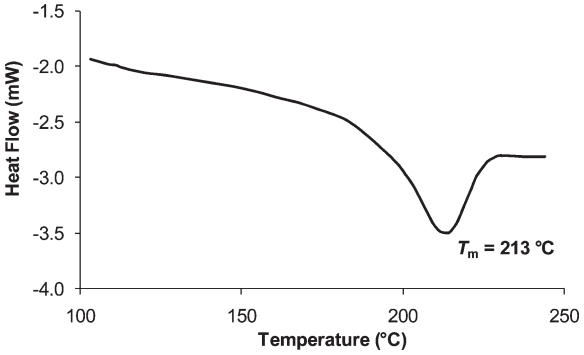

Figure 10. DSC trace of the crystalline stereocomplex prepared by solid-state annealing of POSS end-capped *it*- and *st*-PMMAs in a 1:2 ratio: T_m = 213 °C, ΔH = 15.4 J/g.

diastereomeric random copolymers, *it*-PMMA-*co*-P(MA-POSS) (2.6 mol % MA-POSS, 91% *mm*, entry 2, Table 1) and *st*-PMMA-*co*-P(MA-POSS) (1.9 mol % MA-POSS, 91% *rr*, entry 11, Table 2), showed only a small, negligible endothermic peak of $T_m \approx 198$ °C.

Conclusions

Well-defined MA-POSS end-capped diastereomeric PMMAs with high stereoregularities (94% *it*- and *st*-) have been synthesized using chiral metallocene catalysts at ambient temperature, thanks to the living and stereospecific features of such catalysts. Although

(29) Kawauchi, T.; Kumaki, J.; Yashima, E. *J. Am. Chem. Soc.* **2006**, *128*, 10560–10567.

homopolymerization of the current bulky MA-POSS monomer is not possible by such catalysts, stereospecific statistical copolymerization of MMA with MA-POSS readily produces highly *it*- and *st*-statistical copolymers PMMA-*co*-P(MA-POSS). In the *it*-copolymers, the MA-POSS incorporation can be controlled by the comonomer feed ratio, ranging from a low 2.6 mol % (20 wt %) to a high, maximum 24 mol % (75 wt %). In comparison, the MA-POSS incorporation in the *st*-copolymers is lower with the same comonomer feed ratio, which is attributed to an interesting phenomenon that the *st*-PMMA polymer and the MA-POSS monomer form a crystalline inclusion complex in which the POSS nanocages are encapsulated within the helical *st*-PMMA cavity.

The GPC/LS and DSC studies of the *it*-copolymers having a various level of MA-POSS incorporation have provided evidence for copolymers with high POSS contents (> 20 mol % MA-POSS incorporation) exhibiting interchain association through POSS aggregation and a ~20 °C enhancement in T_g over the pristine *it*-PMMA. Although this inorganic POSS collapse is still evident for the copolymers where the POSS nanocages are statistically distributed along the polymer backbone, their organic methacrylate self-organization is largely disrupted as evidenced by their inability to form a highly crystalline stereocomplex between the diasteromeric *it*- and *st*-copolymers.

Much more versatile nanostructured assemblies have been evidenced by DLS and DSC studies for MA-POSS end-capped diastereomeric PMMAs. First, *it*-PMMA-POSS can form micelle-like core−shell nanostructures of various sizes (R_h = 26−186 nm), through POSS inorganic or methacrylate organic collapse in selective solvents. Second, solution crystallization of the *it*-/*st*-PMMA-POSS blend in a 1/2 ratio, depending on the concentration, generates either stereocomplexes (R_h = 11−31 nm) mostly between two or three polymer chains through organic self-organization of the diastereomeric PMMA chains or larger nanostructured assemblies (e.g., R_h up to 636 nm for the uniform core−shell nanosphere), through synergistic organic PMMA self-organization and inorganic POSS nanocluster aggregation. Third, thermal annealing of the *it*-/*st*-PMMA-POSS blend in a 1:2 ratio can also generate the crystalline stereocomplex with a high T_m of 213 °C.

Acknowledgment. This work was supported by the National Science Foundation (NSF-0718061). We are indebted to Prof. Nancy Levinger for access to the DLS instrument and expert assistance on DLS measurements.